

Article

## Comparative Anti-Infectious Bronchitis Virus (IBV) Activity of (-)-Pinene: Effect on Nucleocapsid (N) Protein

Zhiwei Yang<sup>1,2,†</sup>, Nan Wu<sup>1,2,†</sup>, Yuangang Zu<sup>1,2,\*</sup> and Yujie Fu<sup>1,2,\*</sup>

<sup>1</sup> Key Laboratory of Forest Plant Ecology, Ministry of Education, Northeast Forestry University, Harbin 150040, China

<sup>2</sup> Engineering Research Center of Forest Bio-preparation, Ministry of Education, Northeast Forestry University, Harbin 150040, China; E-Mails: yzws-123@163.com (Z.Y.); bao\_doubao@yahoo.com.cn (N.W.); fuyujie1967@yahoo.com.cn (Y.J.F.)

† These two authors contributed equally to this work.

\* Author to whom correspondence should be addressed; E-Mail: zygorl@vip.hl.cn or fuyujie1967@yahoo.com.cn; Tel.: +86-451-82190535; Fax: +86-451-82190535.

Received: 29 November 2010; in revised form: 23 December 2010 / Accepted: 17 January 2011 / Published: 25 January 2011

---

**Abstract:** In the present study, anti-IBV (infectious bronchitis virus) activities of (-)-pinenes were studied by MTT assay, as well as docking and molecular dynamic (MD) simulations. The  $CC_{50}$  values of (-)- $\alpha$ -pinene and (-)- $\beta$ -pinene were above 10 mM. And the maximum noncytotoxic concentrations ( $TD_0$ ) of (-)- $\alpha$ -pinene and (-)- $\beta$ -pinene were determined as  $7.88 \pm 0.06$  and  $6.09 \pm 0.31$  mM, respectively. The two compounds were found to inhibit IBV with an  $IC_{50}$  of  $0.98 \pm 0.25$  and  $1.32 \pm 0.11$  mM. The MTT assay showed that the inhibitions of (-)-pinenes against IBV appear to occur moderately before entering the cell but are much stronger occur after penetration of the virus into the cell. Molecular simulations indicated that (-)- $\alpha$ -pinene and (-)- $\beta$ -pinene specifically interact with the active site which is located at the N terminus of phosphorylated nucleocapsid (N) protein, with the former being more potent than the latter. The binding energies of them are  $-36.83$  and  $-35.59$  kcal mol<sup>-1</sup>, respectively. Results presented here may suggest that (-)- $\alpha$ -pinene and (-)- $\beta$ -pinene possess anti-IBV properties, and therefore are a potential source of anti-IBV ingredients for the pharmaceutical industry.

**Keywords:** (-)-pinene; anti-IBV activity; MTT; docking; active site

---

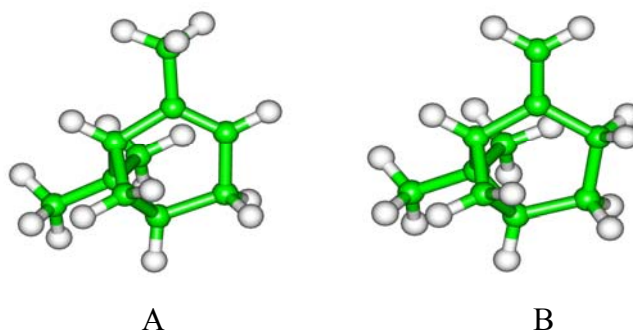
## 1. Introduction

Infectious bronchitis virus (IBV), which belongs to the family Coronaviridae, continues to be one of the most economically important pathogens in the poultry industry. Coronaviruses, which are enveloped viruses with positive sense, 5'capped and 3'polyadenylated RNA genomes, range from 27.6 to 32 kb [1]. Two thirds of the coronavirus genome encodes the replicase activity, including a viral RNA-dependent RNA polymerase (RdRp), helicase, and viral proteinases. The remaining one third of the genome encodes the structural proteins and small group-specific ORFs [1]. Recently, there have been occasional outbreaks of infectious bronchitis (IB) and it remains one of the most important poultry diseases in many countries of the world [2-4]. Consequently, study and exploitation an effective anti-IBV medicine have significant value and broad interest.

IBV has four essential structural proteins: the three membrane proteins, the spike (S), integral membrane (M), and small envelope (E) proteins, and a phosphorylated, nucleocapsid (N) protein. The S protein interacts with cellular receptors and induces cell and viral membrane fusion [5]. The E and M proteins are localized in ER-Golgi intermediate compartment and considered to play critical roles in viral budding [6,7]. N proteins, which interact with viral genomic RNA, forming ribonucleocapsid (RNP) complexes, have been associated with replication and transcription [8-10]. It is a highly immunogenic phosphoprotein also implicated in viral genome replication and in modulating cell signaling pathways. The N-terminal of N-protein (NTD) serves as a functional unit critical for the specific interaction with RNA, where exhibits a U-shaped structure, with two arms rich in basic residues [11]. Additionally, the key functional residues of NTD are highly conserved among coronaviruses between different antigenic groups [12-14]. The N protein has been a major protein target in the exploration of anti-IBV medicine [11-16].

Aromatic and medicinal plants produce essential oils containing both hydrocarbons and oxygenated derivatives. In fact, essential oils have been widely used in traditional medicine. Among others, antibacterial, antifungal, immunomodulatory, antiinflammatory, and antirheumatic activities have been described [17-19]. (-)-Pinenes ( $\alpha$ - and  $\beta$ -) (Figure 1) are major components of turpentine, the byproducts of the pulp making industry. Recent clinical research has shown that they present antimicrobial activities [20,21].

**Figure 1.** Structures of (-)- $\alpha$ -pinene (A) and (-)- $\beta$ -pinene (B).



To the best of our knowledge, the anti-IBV activities of (-)-pinenes ( $\alpha$ - and  $\beta$ -) have not been evaluated yet. Therefore, the aim of the present study was to evaluate the anti-IBV activities of (-)- $\alpha$ -

pinene and (-)- $\beta$ -pinene by MTT assay. Furthermore, explicitly solvated flexible docking and molecular dynamic (MD) methods were applied to investigate the inhibitory mechanisms of the two compounds with the IBV N protein. We anticipate that the insight into the understanding of binding mechanism will be of value in the rational design of IBV inhibitors.

## 2. Results and Discussion

### 2.1. Effects of (-)-pinenes against IBV by MTT assay

Monolayer cultures of Vero cells were grown in 0.005–10 mM (-)-pinene-containing medium and after 72 h of incubation, cell viability was determined by MTT assay. The cytotoxicities of (-)- $\alpha$ -pinene and (-)- $\beta$ -pinene on Vero cells were expressed as  $CC_{50}$  and  $TD_0$ . As shown in Table 1, the  $CC_{50}$  values of (-)- $\alpha$ -pinene and (-)- $\beta$ -pinene were all above 10 mM. And (-)- $\alpha$ -pinene showed higher maximum noncytotoxic concentration ( $TD_0$ ,  $7.88 \pm 0.06$  mM) than (-)- $\beta$ -pinene ( $6.09 \pm 0.31$  mM). These two values were both much higher than that of ribavirin ( $0.78 \pm 0.15$  mM) ( $P < 0.01$ ). These results indicated compared with ribavirin, both (-)- $\alpha$ -pinene and (-)- $\beta$ -pinene possessed lower cytotoxicity on Vero cells. Thus, we could infer that the antiviral effects of (-)- $\alpha$ -pinene and (-)- $\beta$ -pinene were not due to any cytotoxicity.

**Table 1.** Anti-IBV activities of (-)- $\alpha$ -pinene and (-)- $\beta$ -pinene compared with ribavirin.

Compound	$CC_{50}^a$ (mM)	$TD_0^b$ (mM)	IBV (Gray strain)	
			$IC_{50}^c$ (mM)	SI <sup>d</sup>
(-)- $\alpha$ -Pinene	>10.0	$7.88 \pm 0.06$	$0.98 \pm 0.25$	>10.20
(-)- $\beta$ -Pinene	>10.0	$6.09 \pm 0.31$	$1.32 \pm 0.11$	>7.58
Ribavirin	>1.0	$0.78 \pm 0.15$	$0.118 \pm 0.02$	>8.47

Values in this table represent the mean values ( $\pm$ SD) of three independent experiments ( $P < 0.01$ ).

<sup>a, b</sup> Cytotoxic effect was determined by MTT assay.  $CC_{50}$  was the concentration that showed 50% cytotoxic effects in Vero cells.  $TD_0$  was the concentration that showed nontoxic maximum effects in Vero cells; <sup>c</sup> Antiviral activity was determined by MTT assay.  $IC_{50}$  was the concentration that inhibited 50% of IBV replication in Vero cells; <sup>d</sup> The selective index (SI) was calculated as  $CC_{50}/IC_{50}$ .

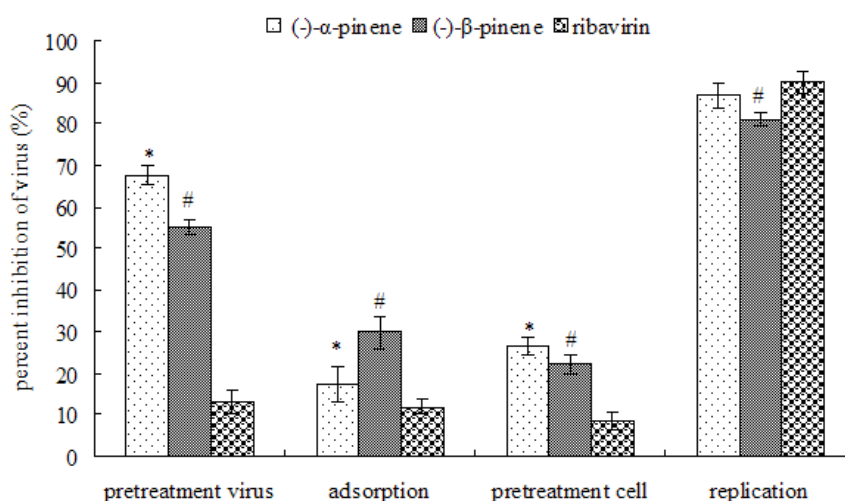
Moreover, the  $IC_{50}$  value of (-)- $\alpha$ -pinene ( $0.98 \pm 0.25$  mM) was somewhat lower than that of (-)- $\beta$ -pinene ( $1.32 \pm 0.11$  mM). Based on the  $IC_{50}$  and  $CC_{50}$  values, the selectivity index (SI) was calculated as >10.20 and >7.58, respectively. It is reported that a SI of 4 or more should be appropriate for an antiviral agent [22]. This suggests that (-)- $\alpha$ -pinene and (-)- $\beta$ -pinene may be judged to have significant anti-IBV activities.

### 2.2. Mode of anti-IBV activity by MTT assay

To identify at which step replication might be inhibited, cells were infected with IBV after preincubation of the cells with ribavirin as positive control or pinenes, pretreatment of the virus with ribavirin or pinenes prior to infection, addition of the synthetic antiviral drug or pinenes during adsorption or after adsorption during the intracellular replication period. In all experiments cells

infected with untreated virus were used as control. The percent reduction was calculated relative to the amount of virus produced in the absence of the drug. As shown in Figure 2, ribavirin showed the maximum antiviral activity when added at a concentration of  $0.78 \pm 0.15$  mM during the replication period with inhibition of the viral replication of  $90.18 \pm 2.80\%$  for IBV. As is commonly known, ribavirin interferes with RNA metabolism required for viral replication [23]. However, no significant effect was detected when ribavirin was used for pretreatment of cells or viruses or when ribavirin was only added during the adsorption phase. Unlike ribavirin, (-)- $\alpha$ -pinene showed the maximum nontoxic antiviral activity when added at a concentration of  $7.88 \pm 0.06$  mM during the replication period with inhibition of the viral replication of  $86.98 \pm 3.04\%$  for IBV, whereas, it also showed inhibition of  $67.64 \pm 2.31\%$  in the pretreatment virus phase. Similarly to (-)- $\alpha$ -pinene, (-)- $\beta$ -pinene also showed significant anti-IBV inhibition during the replication period and pretreatment virus phase, with the inhibition of  $81.02 \pm 1.48\%$  and  $55.41 \pm 1.64\%$ . These results suggested that the inhibitions of (-)-pinenes against IBV appear to moderately occur before entering the cell but much stronger occur after penetration of the virus into the cell. Additionally, biochemical studies indicated that the bioactivity of N protein is an important target for the replication of IBV virus [11,13,16]. Hence, we infer that N protein may be suppressed by (-)-pinenes.

**Figure 2.** Antiviral effects of (-)- $\alpha$ -pinene (7.88 mM), (-)- $\beta$ -pinene (6.09 mM) and ribavirin (0.78 mM) against IBV by incubation at different periods of time during infection.



Cells were pretreated with (-)- $\alpha$ -pinene, (-)- $\beta$ -pinene or ribavirin prior to virus infection (pretreatment cells), viruses were pretreated prior to infection (pretreatment virus), and (-)- $\alpha$ -pinene, (-)- $\beta$ -pinene or ribavirin was added during the adsorption period (adsorption) or after penetration of the viruses into cells (replication). Experiments were repeated independently three times and data presented are the average of 3 experiments. The symbols \* and # indicated very significant difference  $p < 0.01$  with respect to positive control (ribavirin).

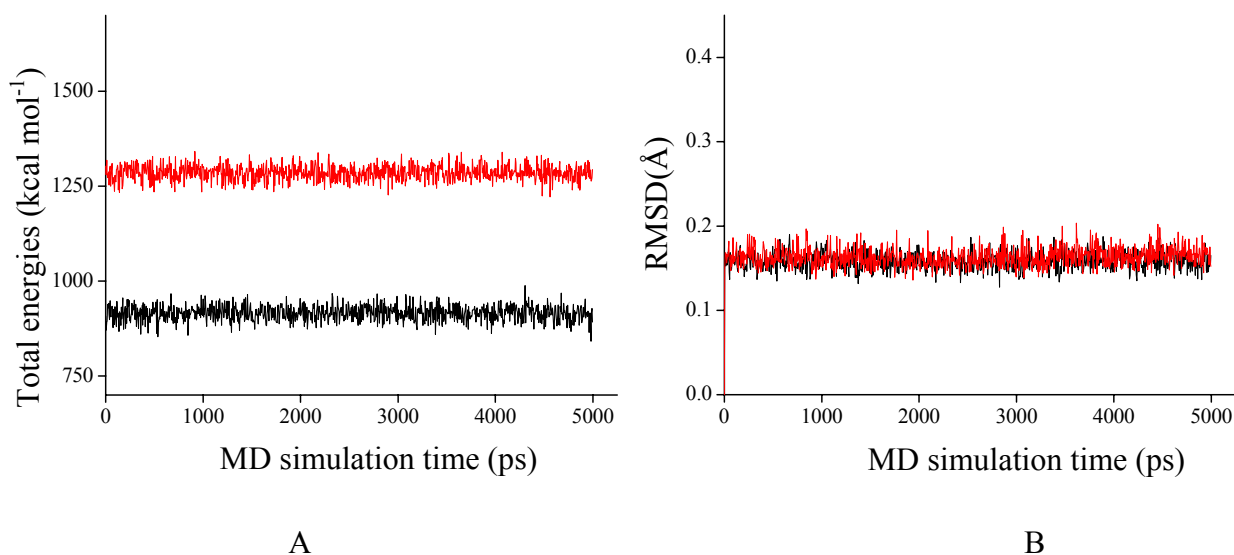
### 2.3. NTD inhibitory activities of (-)-pinenes

In conclusion, (-)- $\alpha$ -pinene and (-)- $\beta$ -pinene both possess anti-IBV properties by hindering the binding process between RNA and IBV N-protein. Our results support for the potential use of (-)- $\alpha$ -pinene and (-)- $\beta$ -pinene in the treatment of IBV infectious disease. Further studies on the anti-IBV mechanism are needed to support this point of view. Therefore, explicit solvent docking and molecular

dynamics (MD) simulations were used to explore the inhibiting mechanisms of (-)- $\alpha$ -pinene and (-)- $\beta$ -pinene with NTD and to try to elucidate the activity differences.

As shown in Figure 3, total energies and backbone-atom RMSDs indicated that the two docked complexes reached equilibrium after about 1,000 ps and remained rather stable afterwards. Accordingly, the geometric and energetic analyses were performed on the average structures of 1,000~5,000 ps MD trajectories. The superposed structures in Figure 4 showed that (-)- $\alpha$ -pinene and (-)- $\beta$ -pinene occupy the proximity space at the RNA binding site of NTD, which is mapped to the loop region on the top of the  $\beta$ -sheet within the protein [11,14]. However, their binding modes differed from each other.

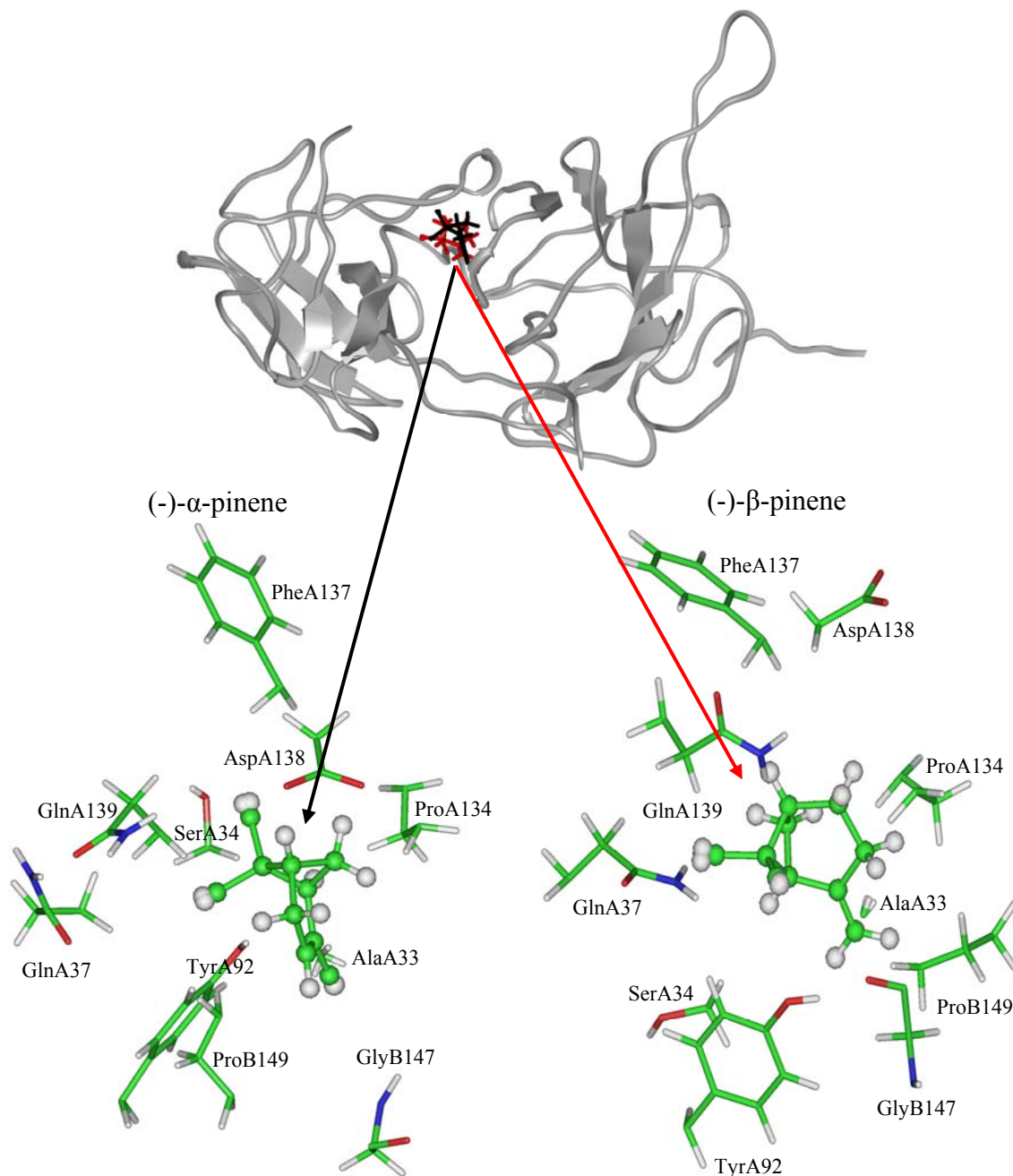
**Figure 3.** The time-evolution total energies (A) and backbone-atom root mean square deviations (RMSD, B) for the docked complexes during the MD simulations.



The values of (-)- $\alpha$ -pinene-NTD and (-)- $\beta$ -pinene-NTD are represented by black and red lines, respectively.

The interaction energy ( $E_{inter}$ ) of (-)- $\alpha$ -pinene with NTD was calculated to be  $-36.83 \text{ kcal mol}^{-1}$ . Van der Waals interactions rather than electrostatic interactions played a dominant role for the binding process, contributing to almost 86%. As Figure 4 shows, the cyclohexene ring of (-)- $\alpha$ -pinene was sandwiched between residues TyrA92 and ProA134 and exerted strong interactions with them. The values ( $E_{sum}$ ) amounted to  $-6.32$  and  $-2.65 \text{ kcal mol}^{-1}$ , respectively (Table 2). Besides, (-)- $\alpha$ -pinene had strong van der Waals interactions ( $E_{vdW}$ ) with residues SerA34, GlnA37, PheA137, AspA138, GlnA139, GlyB147 and ProB149, especially residues PheA137 and ProB149, where the values were equaling  $-2.66$  and  $-2.30 \text{ kcal mol}^{-1}$ , respectively (Figure 4 and Table 2). As these fully or partially conserved residues are key for the RNA bindings [11,14,16], it commendably support a viewpoint that (-)- $\alpha$ -pinene hindered the binding of RNA with NTD, which is in good agreement with the inhibition occurred strongly after penetration of the virus into the host cells.

**Figure 4.** The modeled structures of (-)- $\alpha$ -pinene (black) and (-)- $\beta$ -pinene (red) bound to the nucleocapsid (N) protein.



The nucleocapsid (N) protein is in ribbon. Key residues are represented by stick models. The oxygen, nitrogen, carbon, hydrogen in model are colored in red, blue, green and white, respectively.

Similarly, the binding of (-)- $\beta$ -pinene was mainly stabilized by van der Waals interactions. The interaction energy ( $E_{inter}$ ) of (-)- $\beta$ -pinene with NTD was slightly reduced to  $-35.59 \text{ kcal mol}^{-1}$ , with van der Waals energy ( $E_{vdw}$ ) owning 98% of it. As shown in Figure 4 and Table 2, the strong van der Waals effects were also observed between cyclohexane ring of (-)- $\beta$ -pinene and the residues TyrA92 and ProA134 (Figure 4).

**Table 2.** The vdW, electrostatic and sum interaction energies ( $E_{vdW}$ ,  $E_{ele}$  and  $E_{sum}$ ) involving (-)- $\alpha$ -pinene and (-)- $\beta$ -pinene with the active-site residues of nucleocapsid (N) protein <sup>a</sup>.

Residue	(-)- $\alpha$ -pinene			(-)- $\beta$ -pinene		
	$E_{vdW}$	$E_{ele}$	$E_{sum}$	$E_{vdW}$	$E_{ele}$	$E_{sum}$
AlaA33	—	—	—	-1.81	-0.36	-2.17
SerA34	-1.61	-0.18	-1.79	-3.03	-0.10	-3.13
PheA36	—	—	—	-1.07	-0.50	-1.57
GlnA37	-1.57	0.07	-1.50	-2.22	-0.11	-2.33
TyrA92	-3.86	-2.46	-6.32	-3.45	-0.14	-3.59
ProA134	-2.53	-0.12	-2.65	-2.96	-0.42	-3.38
PheA137	-2.66	0.08	-2.58	-2.00	-0.23	-2.23
AspA138	-1.43	-0.94	-2.37	-2.35	-0.31	-2.66
GlnA139	-2.21	-0.43	-2.64	-2.42	-0.23	-2.65
TyrA140	-1.66	0.08	-1.58	—	—	—
AspB146	-1.00	-0.89	-1.89	—	—	—
GlyB147	-0.77	-0.23	-1.00	-2.47	0.01	-2.46
GlyB148	—	—	—	-1.58	0.55	-1.03
ProB149	-2.30	-0.02	-2.32	-0.63	-0.09	-0.72
TrpB155	-1.85	-0.08	-1.93	-1.57	-0.04	-1.61

<sup>a</sup> Energy units in kcal mol<sup>-1</sup>.

The van der Waals contributions ( $E_{vdW}$ ) of the two residues were calculated to be  $-3.45$  and  $-2.96$  kcal mol<sup>-1</sup>, respectively (Table 2). The maximal binding difference between (-)- $\alpha$ -pinene-NTD and (-)- $\beta$ -pinene-NTD is in that the methylene group (=CH<sub>2</sub>) of (-)- $\beta$ -pinene was oriented towards residue AlaA33. As a result of this situation, the van der Waals contributions ( $E_{vdW}$ ) of residues PheA137 and ProB149 sharply reduced to  $-2.00$  and  $-0.63$  kcal mol<sup>-1</sup>, respectively. It indicated that the binding of RNA may interfere with (-)- $\beta$ -pinene and this effect is lower than that of (-)- $\alpha$ -pinene, consistent with the above experimental data.

Taken together, it is likely that (-)- $\alpha$ -pinene and (-)- $\beta$ -pinene exert their anti-IBV activities through the inhibition of binding process between RNA and IBV N protein, with the former having the higher bioactivity. Therefore, (-)- $\alpha$ -pinene and (-)- $\beta$ -pinene should be potential lead compounds in the developing the anti-IBV agents. Further studies on the anti-IBV drugs are urgently needed to support this point of view.

### 3. Experimental

#### 3.1. Materials

(-)- $\alpha$ -Pinene, (-)- $\beta$ -pinene and ribavirin were obtained from Sigma Chemical Co. (St. Louis, MO, USA) and was stored in glass vials with Teflon sealed caps at  $-20 \pm 0.5$  °C in the absence of light.

#### 3.2. Cell cultures

Vero-E6 (African green monkey kidney cells) was purchased from Harbin Veterinary Research Institute (Harbin, P. R. China). The cells were grown in monolayer culture with Dulbecco's modified

Eagle's medium (DMEM) supplemented with 10% fetal calf serum (FCS), 100 U/mL penicillin and 100 µg/mL streptomycin. The monolayers were removed from their plastic surfaces and serially passaged whenever they became confluent. Cells were plated out onto 96-well culture plates for cytotoxicity and anti-IBV assays, and propagated at 37 °C in an atmosphere of 5 % CO<sub>2</sub>.

### 3.3. Viruses

The IBV Gray strain was purchased from National Control Institute of Veterinary Bioproducts and Pharmaceuticals (Beijing, P. R. China). Virus was routinely grown on Vero-E6 cells. IBV-Gray stock cultures were prepared from supernatants of infected cells and stored at −80 °C.

### 3.4. Cytotoxicity assay

The cellular toxicity of (-)-α-pinene and (-)-β-pinene on Vero-E6 cells was assessed by the MTT method [24]. Briefly, cells were seeded on a microtiter plate in the absence or presence of various concentrations (10 mM – 0.005 mM) of (-)-α-pinene and (-)-β-pinene for eight replicates and incubated at 37 °C in a humidified atmosphere of 5% CO<sub>2</sub> for 72 h. The supernatants were discarded, washed with PBS twice and MTT reagent (5 mg/mL in PBS) was added to each well, after incubated at 37 °C for 4 h, remove the supernatants, then 200 µL DMSO was added and incubated at 37 °C for another 30 min. After that the plates were read on an ELISA reader (Thermo Molecular Devices Co., Union City, USA) at 570/630 nm. The mean OD of the cell control wells was assigned a value of 100%. The maximal non-toxic concentration (TD<sub>0</sub>) and 50% cytotoxic concentration (CC<sub>50</sub>) were calculated by linear regression analysis of the dose-response curves generated from the data.

### 3.5. Anti-IBV activity

Inhibition of virus replication was measured by MTT method [25]. Serial dilution of the treated virus was adsorbed to the cells for 1 h at 37 °C. The residual inoculum was discarded and infected cells were added with DMEM containing 2% FCS. Each assay was performed in eight replicates. After incubation for 72 h at 37 °C, the cultures were measured by MTT method as described above. The concentration of (-)-α-pinene, (-)-β-pinene and ribavirin which inhibited virus numbers by 50% (IC<sub>50</sub>) was determined from dose-response curves.

### 3.6. Mode of anti-IBV activity

Cells and viruses were incubated with (-)-α-pinene or (-)-β-pinene at different stages during the viral infection cycle in order to determine the mode of antiviral action [24]. Cells were pretreated with (-)-α-pinene or (-)-β-pinene before viral infection, viruses were incubated with (-)-α-pinene or (-)-β-pinene before infection and cells and viruses were incubated together with (-)-α-pinene or (-)-β-pinene during adsorption or after penetration of the virus into the host cells. (-)-α-pinene or (-)-β-pinene was always used at the nontoxic concentration. Cell monolayers were pretreated with (-)-α-pinene or (-)-β-pinene prior to inoculation with virus by adding (-)-α-pinene or (-)-β-pinene to the culture medium and incubation for 1h at 37 °C. The compound was aspirated and cells were washed immediately before the IBV inoculum was added. For pretreatment virus, IBV were incubated in medium containing (-)-α-

pinene or (-)- $\beta$ -pinene for 1h at room temperature prior to infection of Vero-E6 cells. For analyzing the anti-IBV inhibition during the adsorption period, the same amount of IBV was mixed with the drug and added to the cells immediately. After 1h of adsorption at 37 °C, the inoculum was removed and DMEM supplemented with 2% FCS were added to the cells. The effect of (-)- $\alpha$ -pinene or (-)- $\beta$ -pinene (or ribavirin) against IBV was also tested during the replication period by adding it after adsorption, as typical performed in anti-IBV susceptibility studies. Each assay was run in eight replicates. Ribavirin was used as a positive control.

### 3.7. Flexible docking and MD simulations

The protein receptor N-terminal domain of N-protein (PDB ID: 2GEC) [11] from the RCSB Protein Data Bank was taken without the crystal water molecules [14]. For convenience, it is named as NTD throughout this work. The geometries and partial atomic charges of (-)- $\alpha$ -pinene and (-)- $\beta$ -pinene (Figure 1) were taken by applying the BFGS algorithm (Discover 3.0 module) [26], with the consistent-valence force-field (CVFF). The convergence criterion was set to 0.01 kcal mol<sup>-1</sup> Å<sup>-1</sup>. Demonstrated by previous literatures [14,27-29], the explicitly solvated flexible docking and molecular dynamics (MD) simulations were performed by the general and popular protocols in the InsightII 2005 software packages [30] on Linux workstations. The MD trajectories were generated using a 1.0-fs time step for a total of 5,000 ps, saved at 5.0-ps intervals. The interaction energies of the compounds with NTD and the respective residues at the NTD active site were calculated by the Docking module [31], over the 1,000~5,000 ps MD trajectories. More calculated details are referred elsewhere [27,29].

### 3.8. Statistical analysis

All results are expressed as mean values  $\pm$  standard deviations (SDs) (n = 3). The significance of difference was calculated by one-way analysis of variance, and values  $p < 0.01$  were considered to be significant.

## 4. Conclusions

The current study demonstrated that the certain anti-IBV activity as well as the inhibition of binding process between RNA and IBV N protein of (-)- $\alpha$ -pinene and (-)- $\beta$ -pinene. Further pharmacological investigations are necessary to provide evidence about the anti-IBV mechanism of these two compounds.

## Acknowledgements

The authors gratefully acknowledge the financial supports by Key Program for Science and Technology Development of Harbin (2009AA3BS083), National Natural Science Foundation of China (30770231), Heilongjiang Province Science Foundation for Excellent Youths (JC200704), Agricultural Science and Technology Achievements Transformation Fund Program (2009GB23600514), Key Project of Chinese Ministry of Education (108049), Project for Distinguished Teacher Abroad, Chinese Ministry of Education (MS2010DBLY031), Fundamental Research Funds for the Central Universities (DL09EA04), Special Fund of Forestry Industrial Research for Public Welfare of China

(201004040) and the Cultivated Funds of Excellent Dissertation of Doctoral Degree Northeast Forestry University (grap09).

## References and Notes

1. Lai, M.M.; Cavanagh, D. The molecular biology of coronaviruses. *Adv. Virus. Res.* **1997**, *48*, 1-100.
2. Reynolds, J.E.F. *Martindale the Extra Pharmacopoeia*; Royal Pharmaceutical Society of Great Britain: London, UK, 1996; Volume 31, p. 342.
3. Pei, J.; Briles, W.E.; Collisson, E.W. Memory T cells protect chicks from acute infectious bronchitis virus infection. *Virology* **2003**, *306*, 376-384.
4. Mondal, S.P.; Cardona, C.J. Comparison of four regions in the replicase gene of heterologous infectious bronchitis virus strains. *Virology* **2004**, *324*, 238-248.
5. Bosch, B.J.; van der Zee, R.; de Haan, C.A.; Rottier, P.J. The coronavirus spike protein is a class I virus fusion protein: structural and functional characterization of the fusion core complex. *J. Virol.* **2003**, *77*, 8801-8811.
6. de Haan, C.A.; Kuo, L.; Masters, P.S.; Vennema, H.; Rottier, P.J. Coronavirus particle assembly: Primary structure requirements of the membrane protein. *J. Virol.* **1998**, *72*, 6838-6850.
7. Fischer, F.; Stegen, C.F.; Masters, P.S.; Samsonoff, W.A. Analysis of constructed E gene mutants of mouse hepatitis virus confirms a pivotal role for E protein in coronavirus assembly. *J. Virol.* **1998**, *72*, 7885-7894.
8. Robbins, S.G.; Frana, M.F.; McGowan, J.J.; Boyle, J.F.; Holmes, K.V. RNA-binding proteins of coronavirus MHV: Detection of monomeric and multimeric N protein with an RNA overlay-protein blot assay. *Virology* **1986**, *150*, 402-410.
9. Compton, S.R.; Rogers, D.B.; Holmes, K.V.; Fertsch, D.; Remenick, J.; McGowan, J.J. *In vitro* replication of mouse hepatitis virus strain A59. *J. Virol.* **1987**, *61*, 1814-1820.
10. Baric, R.S.; Nelson, G.W.; Fleming, J.O.; Deans, R.J.; Keck, J.G.; Casteel, N.; Stohlman, S.A. Interactions between coronavirus nucleocapsid protein and viral RNAs: Implications for viral transcription. *J. Virol.* **1988**, *62*, 4280-4287.
11. Jayaram, H.; Fan, H.; Bowman, B.R.; Ooi, A.; Jayaram, J.; Collisson, E.W.; Lescar, J.; Prasad, B.V. X-ray structures of the N- and C-terminal domains of a coronavirus nucleocapsid protein: Implications for nucleocapsid formation. *J. Virol.* **2006**, *80*, 6612-6620.
12. Saif, L.J. Coronavirus immunogens. *Vet. Microbiol.* **1993**, *37*, 285-297.
13. Tan, Y.W.; Fang, S.; Fan, H.; Lescar, J.; Liu, D.X. Amino acid residues critical for RNA-binding in the N-terminal domain of the nucleocapsid protein are essential determinants for the infectivity of coronavirus in cultured cells. *Nucleic. Acids. Res.* **2006**, *34*, 4816-4825.
14. Yang, Z.W.; Wu, N.; Fu, F.J.; Yang, G.; Wang, W.; Zu, Y.G.; Efferth, T. Anti-infectious bronchitis virus (IBV) activity of 1,8-cineole: Effect on nucleocapsid (N) protein. *J. Biomol. Struct. Dyn.* **2010**, *28*, 323-330.
15. Nelson, G.W.; Stohlman, S.A.; Tahara, S.M. High affinity interaction between nucleocapsid protein and leader/intergenic sequence of mouse hepatitis virus RNA. *J. Gen. Virol.* **2000**, *81*, 181-188.
16. Fan, H.; Ooi, A.; Tan, Y.W.; Wang, S.; Fang, S.; Liu, D.X.; Lescar, J. The nucleocapsid protein of coronavirus infectious bronchitis virus: crystal structure of its N-terminal domain and multimerization properties. *Structure* **2005**, *13*, 1859-1868.

17. Saller, R.; Reichling, J.; Hellenbrecht, D. *Phytotherapie Klinische, Pharmakologische und Pharmazeutische Grundlagen*; Haug-Verlag: Heidelberg, Germany, 1995.
18. Hammer, K.A.; Carson, C.F.; Riley, T.V. Antimicrobial activity of essential oils and other plant extracts. *J. Appl. Microbiol.* **1999**, *86*, 985-990.
19. Reichling, J.; Wildi, E.; Wink, M. *Trends in Medicinal Plant Research*; Romneya-Verlag: Dossenheim, Germany, 2001.
20. Mourey, A.; Canillac, N. Anti-*Listeria monocytogenes* activity of essential oils components of conifers. *Food Control* **2002**, *13*, 289-292.
21. Hyatt, D.C.; Croteau, R. Mutational analysis of a monoterpene synthase reaction: Altered catalysis through directed mutagenesis of (-)-pinene synthase from *Abies grandis*. *Arch. Biochem. Biophys.* **2005**, *439*, 222-233.
22. Tsuchiya, Y.; Shimizu, M.; Hiyama, Y.; Itoh, K.; Hashimoto, Y.; Nakayama, M.; Horie, T.; Morita, N. Antiviral activity of natural occurring flavonoids *in vitro*. *Chem. Pharm. Bull (Tokyo)* **1985**, *33*, 3881-3886.
23. Leysen, P.; Balzarini, J.; De Clercq, E.; Neyts, J. The predominant mechanism by which ribavirin exerts its antiviral activity *in vitro* against flaviviruses and paramyxoviruses is mediated by inhibition of IMP dehydrogenase. *J. Virol.* **2005**, *79*, 1943-1947.
24. Schnitzler, P.; Schneider, S.; Stintzing, F.C.; Carle, R.; Reichling, J. Efficacy of an aqueous *Pelargonium sidoides* extract against herpesvirus. *Phytomedicine* **2008**, *15*, 1108-1116.
25. Okamoto, M.; Okamoto, T.; Baba, M. Inhibition of human immunodeficiency virus type 1 replication by combination of transcription inhibitor K-12 and other antiretroviral agents in acutely and chronically infected cells. *Antimicrob. Agents Chemother.* **1999**, *43*, 492-497.
26. Head, J.D.; Zerner, M.C. A Broyden—Fletcher—Goldfarb—Shanno optimization procedure for molecular geometries. *Chem. Phys. Lett.* **1985**, *122*, 264-270.
27. Yang, Z.W.; Yang, G.; Zu, Y.G.; Fu, Y.J.; Zhou, L.J. The conformational analysis and proton transfer of the neuraminidase inhibitors: a theoretical study. *Phys. Chem. Chem. Phys.* **2009**, *11*, 10035-10041.
28. Yang, Z.W.; Zu, Y.G.; Wu, X.M.; Liu, C.B.; Yang, G. A computational investigation on the interaction mechanisms of neuraminidases and 3-(3-pentyloxy)benzoic acid. *Acta Chimica Sinica.* **2010**, *14*, 1370-1378.
29. Yang, Z.; Nie, Y.; Yang, G.; Zu, Y.; Fu, Y.; Zhou, L. Synergistic effects in the designs of neuraminidase ligands: Analysis from docking and molecular dynamics studies. *J. Theor. Biol.* **2010**, *267*, 363-374.
30. Accelrys Inc. *InsightII, Version 2005*. Accelrys Inc.: San Diego, CA, USA.
31. Accelrys Inc. *Affinity User Guide*. Accelrys Inc.: San Diego, CA, USA, 2005.

*Sample Availability:* Samples of (-)- $\alpha$ -pinene and (-)- $\beta$ -pinene are available on request from the authors.